

Analysis of Inverse-Prandtl of Dissipation in Standard k- ϵ Turbulence Model for Predicting Flow Field of Crossflow Wind Turbine


 Open
Access

Gun Gun R Gunadi^{1,2,*}, Ahmad Indra Siswantara¹, Budiarmo¹, Hariyotejo Pujowidodo^{1,3}, Candra Damis Widiawaty^{1,2}, Dendy Adanta⁴

¹ Department of Mechanical Engineering, Faculty of Engineering, Universitas Indonesia, Kampus UI Depok, Depok 16424, Indonesia

² Department of Mechanical Engineering, Politeknik Negeri Jakarta, Depok 16424, Indonesia

³ Center for Thermodynamics, Engine, and Propulsion, BPPT, Serpong, Tangerang Selatan 15314, Indonesia

⁴ Department of Mechanical Engineering, Faculty of Engineering, Universitas Sriwijaya, Indralaya 30662, South Sumatera, Indonesia

ARTICLE INFO

Article history:

Received 20 February 2020

Received in revised form 18 April 2020

Accepted 22 April 2020

Available online 30 April 2020

ABSTRACT

The analysis of the turbulence model on turbulent flow in certain objects is important to optimize the numerical simulation. To simulate rotating flow in crossflow turbine, the numerical accuracy of the Renormalization Group (RNG) k- ϵ model has better results than the standard k- ϵ model. To improve predictions of the standard k- ϵ turbulent model can be done by adjusting the constant value. This study discusses the effect of constant inverse-Prandtl number in dissipation equation (σ_ϵ) on the standard k- ϵ turbulent model toward the prediction of the flow field. Case studies of the effect of σ_ϵ constant on flow field prediction were carried out in crossflow wind turbines. The σ_ϵ constant values examined are 1, 1.2, 1.4 and 1.5. Based on the results, there is a significant influence on the flow field prediction in a crossflow wind turbine. This shows that to improve the prediction of the standard k- ϵ turbulent model can be done by testing the σ_ϵ constant values.

Keywords:

Crossflow wind turbine; CFD; standard k- ϵ ; turbulent model; inverse-Prandtl of dissipation

Copyright © 2020 PENERBIT AKADEMIA BARU - All rights reserved

1. Introduction

The computational fluid dynamics (CFD) method has been used widely in the initial analysis of experiments since it has saved time and costs [1-2]. The CFD method can easily vary the flow parameters and geometry to get the desired results [3]. The CFD results are influenced by flow field approaches to predict turbulent flow [4]. In turbulent flow, the properties of the fluid show random and chaotic behavior [5]. The CFD results on turbulent flow in certain objects are influenced by the selection of the right turbulent model [6].

* Corresponding author.

E-mail address: gungun.rg@mesin.pnj.ac.id (Gun Gun R Gunadi)

There are two flow field approaches to predict turbulent flow that is often used: Reynolds Average Navier-Stokes (RANS) and Reynolds Stress Model (RSM). However, the RANS is more often used because of the moderate computing power and fairly good accuracy even though it is not as accurate as RSM [7]. In RANS, the most widely used is the standard $k-\epsilon$ and Re-normalization Group (RNG) $k-\epsilon$ turbulent model, because quite stable and extensively proven used for technical analysis in the industry [8].

The standard $k-\epsilon$ turbulent model is often used in the industrial, but it is not appropriate to simulate rotating flow, large stain flow, open channel flow, and fully developed flow in non-circular channels [9]. Whereas the RNG $k-\epsilon$ turbulent model is an improvement in the prediction of the standard $k-\epsilon$ turbulent model [10]. Yakhot and Orszag constructed the RNG $k-\epsilon$ model from the statistical theory of the renormalization group [11]. The prediction improvement of the RNG $k-\epsilon$ model is done by adding some equations such as the term of the swirl effect of turbulence; the differential formula for effective viscosity; and the analytical formula for the turbulent Prandtl number [11-12].

To improve predictions of the standard $k-\epsilon$ turbulent model, an alternative that can be done is constant value must be adjusted to the case to be examined. Since the constants in the standard $k-\epsilon$ turbulent model are obtained by testing, so that it is appropriate only for the cases tested [8]. So, the constants in the standard $k-\epsilon$ turbulent model for flow in a pipe, flow in the airfoil, enlarged flow field and or crossflow turbines are different. For the case of crossflow turbines, several flow field characteristics have been carried out where this is to propose an appropriate standard $k-\epsilon$ turbulent model constants. Klemm *et al.*, [13] analyzed flow dynamics in crossflow wind turbines using CFD method with standard $k-\epsilon$ turbulent model and default constant. Based on the results, the standard $k-\epsilon$ turbulent model is a good agreement to predict the flow field and performance of crossflow wind turbines. Since the standard $k-\epsilon$ turbulent model able to predict the throughflow zones and recirculation zones that occur inside of runner with precision. Improvement in the prediction of the standard $k-\epsilon$ turbulent model for case crossflow wind turbines has been carried out by changing the constant value [14]. The improvement of the standard $k-\epsilon$ model has been done by various inverse-Prandtl of kinetic (σ_k) 0.8, 0.9, 1, 1.1 and 1.2. The study was conducted at σ_k because turbulent kinetic energy in crossflow wind turbines dominates the flow field than the dissipation rate. So, more accurately it is determining the σ_k value, the prediction of flow field and performance of the crossflow wind turbines will be accurate. From the results, the change in σ_k on the standard $k-\epsilon$ model for the crossflow wind turbine has an influence [14]. Thus, σ_k has contributed to the predicted cascade of energy.

The flow of recirculation in the crossflow turbine causes the mixing process between large scale and small-scale eddies. The mixing process of the eddies will dissipate into heat due to its friction. σ_k affects the prediction of turbulence kinetic energy (k) transport, therefore it is assumed that the inverse-Prandtl of dissipation (σ_ϵ) will also affect the prediction of dissipation rate (ϵ) transport. So, the analysis of σ_ϵ in the standard $k-\epsilon$ turbulence model to analyze flow characteristics in the crossflow turbine is also needed for the study. Thus, this study analyzes the standard $k-\epsilon$ model with various σ_ϵ to improve the accuracy for predict flow field and performance of the crossflow wind turbine.

2. Methodology

2.1 Geometry

The crossflow wind turbines domain in the simulation as shown in Figure 1, with details geometry shown in Table 1.

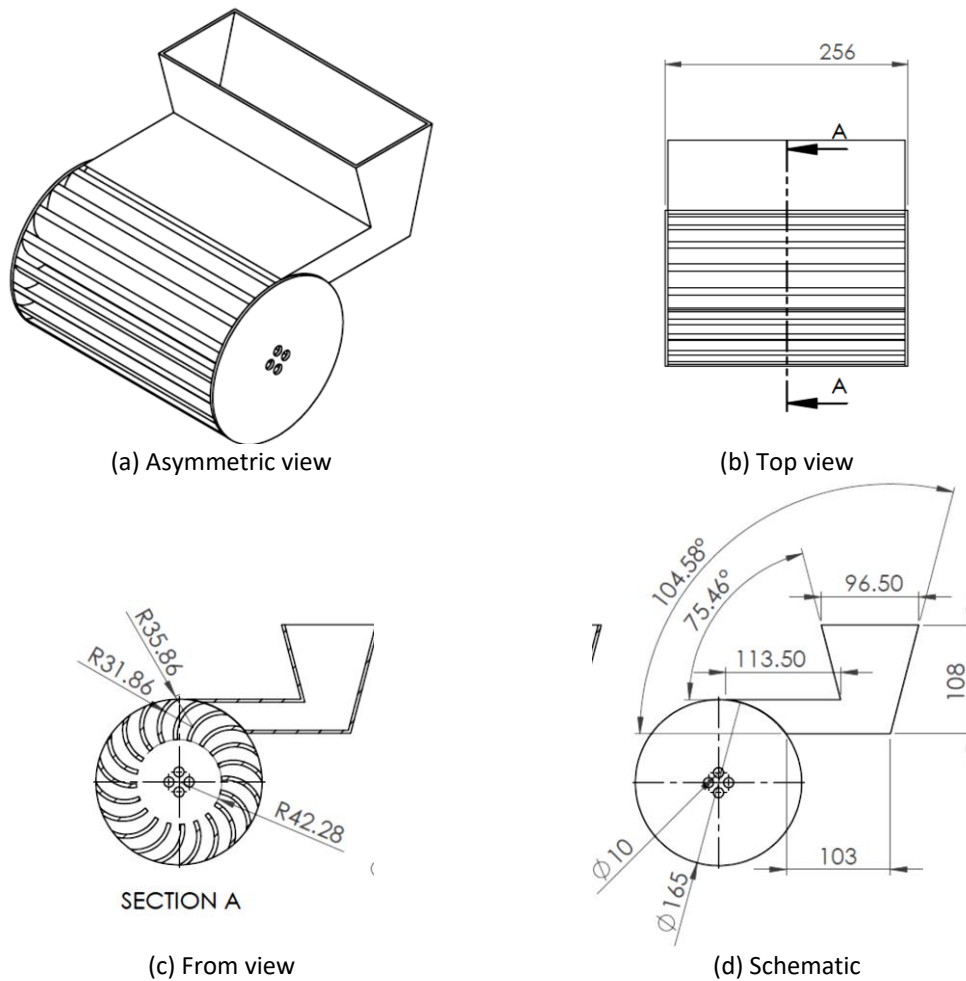


Fig. 1. The crossflow wind turbine

Table 1
The geometry of the crossflow wind turbine

Design Parameter	Value	Design Parameter	Value
Outer diameter	165 mm	Inner diameter	84.56 mm
Number of blades	20	Angle of attack	15°
Blade's inlet angle	35°	Blade's outlet angle	90°
Blade's curve radius	31.86 mm	Nozzle initial height	28 mm

2.2 Turbulence Models

This simulation study began by using the turbulent model standard k-ε and RNG k-ε to determine whether these two models are appropriate for predicting the dynamics parameters of flow on the crossflow turbine blade. This simulation is continued by modifying the standard k-ε model by varying σ_ϵ .

The governing equations of the standard k-ε model show in Eqs. (1) and (2). Eqs. (1) and (2) for the turbulence kinetic energy (k) and the dissipation rate (ε) transport equation, respectively [15].

$$\frac{\partial}{\partial t}(\rho k) + \frac{\partial}{\partial x_j}(\rho k u_j) = \frac{\partial}{\partial x_j} \left[\left(\mu + \frac{\mu_t}{\sigma_k} \right) \frac{\partial k}{\partial x_j} \right] + G_k + G_B - \rho \epsilon + Y_m + S_k \quad (1)$$

$$\frac{\partial(\rho\varepsilon)}{\partial t} + \frac{\partial}{\partial x_j}(\rho\varepsilon u_j) = \frac{\partial}{\partial x_j} \left[\left(\mu + \frac{\mu_t}{\sigma_\varepsilon} \right) \frac{\partial \varepsilon}{\partial x_j} \right] + C_{1\varepsilon} \frac{\varepsilon}{k} (G_k + C_{3\varepsilon} G_B) - C_{2\varepsilon} \rho \frac{\varepsilon^2}{k} + S_\varepsilon \quad (2)$$

where:

$$\mu_t = \rho C_\mu \frac{k^2}{\varepsilon} \quad (3)$$

where C_μ , σ_k , σ_ε , $C_{1\varepsilon}$ and $C_{2\varepsilon}$ are constants with the value C_μ of 0.09, σ_k of 1, $C_{1\varepsilon}$ of 1.44, $C_{2\varepsilon}$ of 1.92, σ_ε of 1.1, 1.2, 1.3, 1.4 and 1.5, respectively.

Due to the RNG k- ε model has better accuracy for rotating flow [11-12], so this model is used as a reference to determine the standard k- ε model error.

The turbulence kinetic energy (k) and the dissipation rate (ε) transport equation are further equations in the RNG k- ε model for turbulent flow as shown in Eqs. (4) and (5), respectively [16].

$$\frac{\partial(\rho k)}{\partial t} + \frac{\partial}{\partial x_i}(\rho k u_i) = \frac{\partial}{\partial x_j} \left(\alpha_\varepsilon \mu_{eff} \frac{\partial k}{\partial x_j} \right) + G_k + G_B - \rho \varepsilon + Y_m + S_k \quad (4)$$

$$\frac{\partial(\rho\varepsilon)}{\partial t} + \frac{\partial}{\partial x_i}(\rho\varepsilon u_i) = \frac{\partial}{\partial x_j} \left(\alpha_\varepsilon \mu_{eff} \frac{\partial \varepsilon}{\partial x_j} \right) + C_{1\varepsilon} \frac{\varepsilon}{k} (G_k + C_{3\varepsilon} G_B) - C_{2\varepsilon}^* \rho \frac{\varepsilon^2}{k} - R_\varepsilon + S_\varepsilon \quad (5)$$

where:

$$C_{2\varepsilon}^* = C_{2\varepsilon} + \frac{C_\mu \eta^3 (1 - \eta/\eta_0)}{1 + \beta \eta^3} \quad (6)$$

$$\eta = Sk/\varepsilon \text{ and } S = (2S_{ij}S_{ij})^{1/2} \quad (7)$$

where C_μ , σ_k , σ_ε , $C_{1\varepsilon}$, $C_{2\varepsilon}$, η_0 and β are constants with the value C_μ of 0.0845, σ_k of 1.393, σ_ε of 1.393, $C_{1\varepsilon}$ of 1.42, $C_{2\varepsilon}$ of 1.68, η_0 of 4.38 and β of 0.012, respectively.

2.3 Mesh Independency Test

Mesh independence is determined by the Grid Convergence Index (GCI) analysis. The GCI is done to determine the percentage of errors mesh size pairs [17]; GCI to get the medium mesh is

$$GCI_{12} = F_s \times \left| \frac{1}{\tau_{fine}} \frac{\tau_{medium} - \tau_{fine}}{r_{12}^{p_n - 1}} \right| \times 100\% \quad (8)$$

where F_s is a safety factor with a value of 1.25. Analysis of the convergence observed (p_n) was carried out using Eq. (9). The Richardson's extrapolation ($P_{rh} = 0$) was applied for fine to medium mesh category, to get an estimated value of velocity recovery at zero grid distance using Eq. (11) [17]:

$$p_{n+1} = \ln \left[\left(\frac{\tau_{coarse} - \tau_{medium}}{\tau_{medium} - \tau_{fine}} (r_{12}^{p_n} - 1) \right) + r_{12}^{p_n} \right] / \ln(r_{12} \cdot r_{23}) \quad (9)$$

$$Pr_{h=0} = \tau_{fine} - \left(\frac{\tau_{medium} - \tau_{fine}}{r_{12}^{p_{n+1} - 1}} \right) \quad (10)$$

$$r_{12} = \left(\frac{\tau_{medium}}{\tau_{fine}} \right)^{0.5} \quad (11)$$

where r_{12} is the grid refinement ratio and M is the mesh number.

The results of mesh independence are shown in Table 2. Mesh number used is 59364 elements. The mesh used is a structured cell with number of mesh $204 \times 97 \times 2$ (see Figure 2).

Table 2
Mesh independency test results

Number of mesh	Torque, τ	r	GCI
44928	7.24 N.m	1.15	-
54000	7.14 N.m	1.05	2.04%
59364	7.11 N.m	1	1.50%

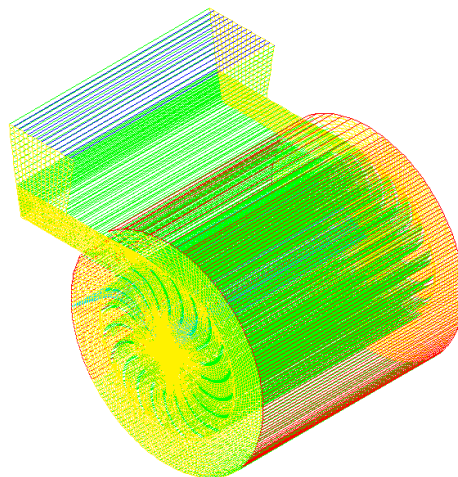


Fig. 2. Visualization of Mesh

2.4 Boundary Conditions

There are several boundary conditions applied in this simulation. The inlet velocity used was 50 m/s. Angular velocity of the runner of 314.286 rad/s. It is assumed there is no influence of body force ($G_y = 0$). The fluid that flows is air. The simulation carried out was transient in the Δt area of 0.0001 s. This value is used based on previous studies, where Δt 0.0001 s can reasonably well represent the change in the flow field that occurs.

3. Results

The validation of this simulation by evaluating the velocity contours. The velocity contours of simulations results are compared to secondary data (as shown in Figure 4 [8,13]). The simulation results are said to be valid is if velocity contour can visualize the phenomenon of throughflow and recirculation flow. From Figure 3, the simulation results with the RNG k- ϵ model visualize the phenomenon of throughflow and recirculation flow, which is similar to the previous study [8,13]. Therefore, this simulation can be categorized as valid.

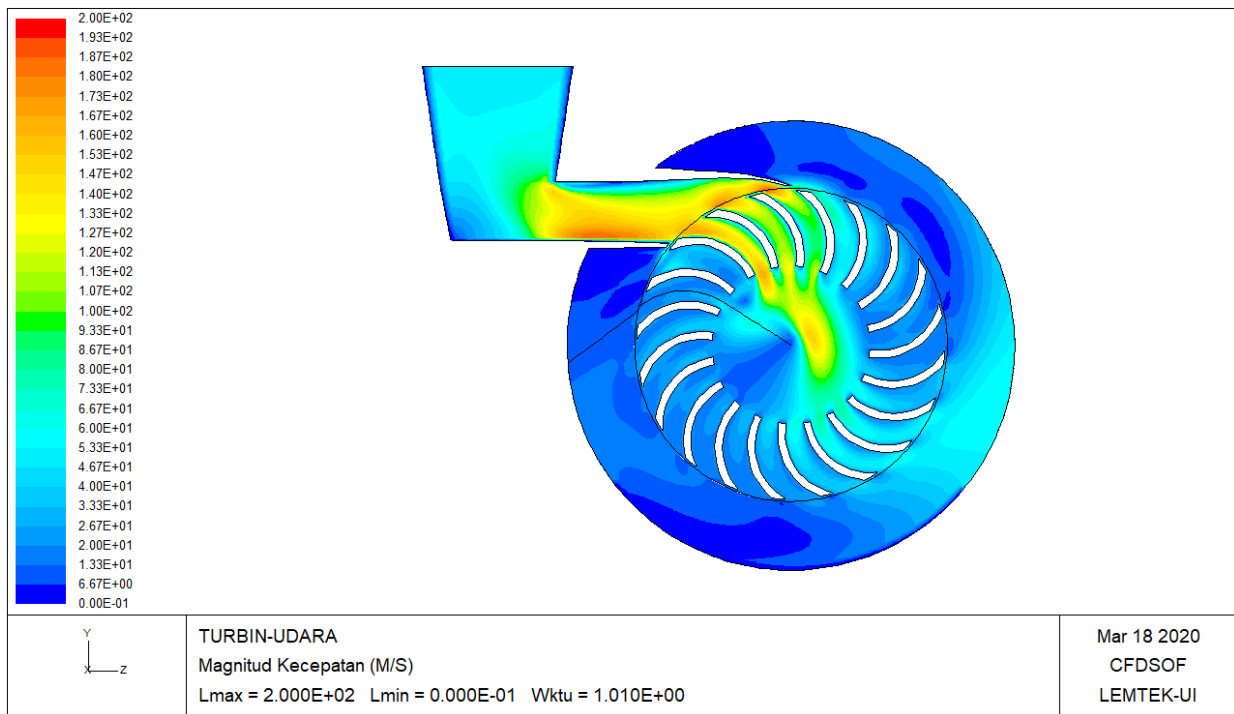
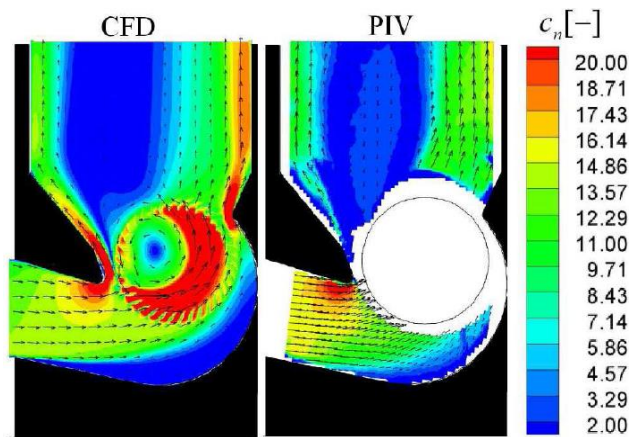
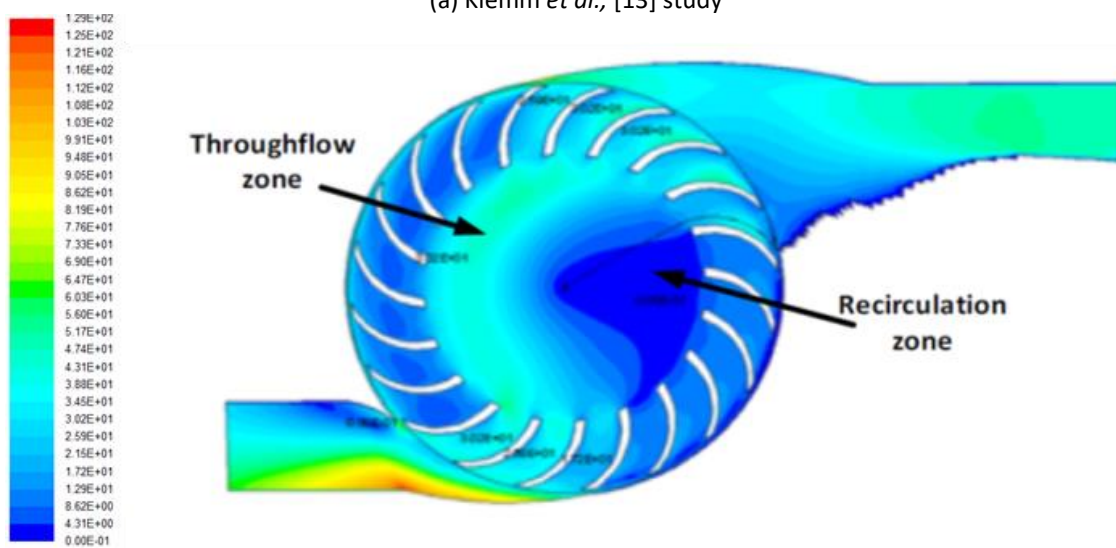


Fig. 3. The velocity contours of the crossflow wind turbine



(a) Klemm *et al.*, [13] study



(b) Darmawan *et al.*, [8] study

Fig. 4. Velocity distribution

The simulation results with the RNG k- ϵ model are shown in Figures 5 to 8. The results Figure 5 shows the velocity magnitude contours in the runner. Based on Figure 5, it can be seen that the vortex recirculation and throughflow occur in the middle of the runner as indicated by the arrow. The forced vortex occurs in the throughflow zone where the fluid passes the first inlet to the second inlet. At the other zones with less fluid concentration forms the eccentric vortex in the recirculation flow. Large eccentric vortices in the middle of the runner can reduce the kinetic energy transfer to mechanical energy due to obstruction of the blade channels.

Figure 5 presented that the highest velocity occurs at the inlet side of the first stage blade, which will produce the highest momentum. High turbulence in the first stage blade is created by the velocity magnitude gradient between the inlet and outlet of the blade. This phenomenon is confirmed by the turbulent kinetic energy contours shown in Figure 6.

The simulation results of the contour of the absolute total pressure are shown in Figure 7. Figure 7 presented that the distribution of absolute total pressure is uneven in the first stage blade area causing random and fluctuating flow dynamics. The dynamics of the flow will generate turbulence in the blade area. This is in accordance with the contour of the turbulent dissipation rate as shown in Figure 8. Figure 8 demonstrated that in the surface area of the first stage blade inlet occurs a fairly large turbulent dissipation rate, this is due to the occurrence of small eddies.

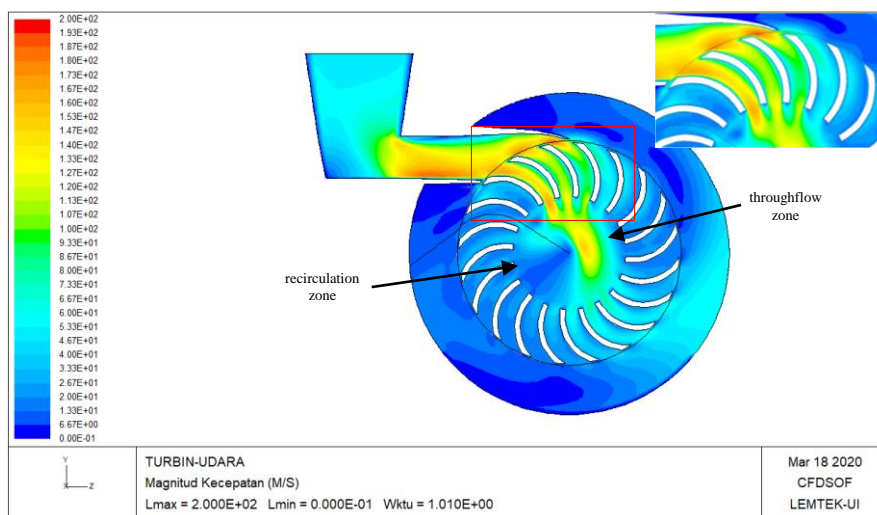


Fig. 5. The velocity contours

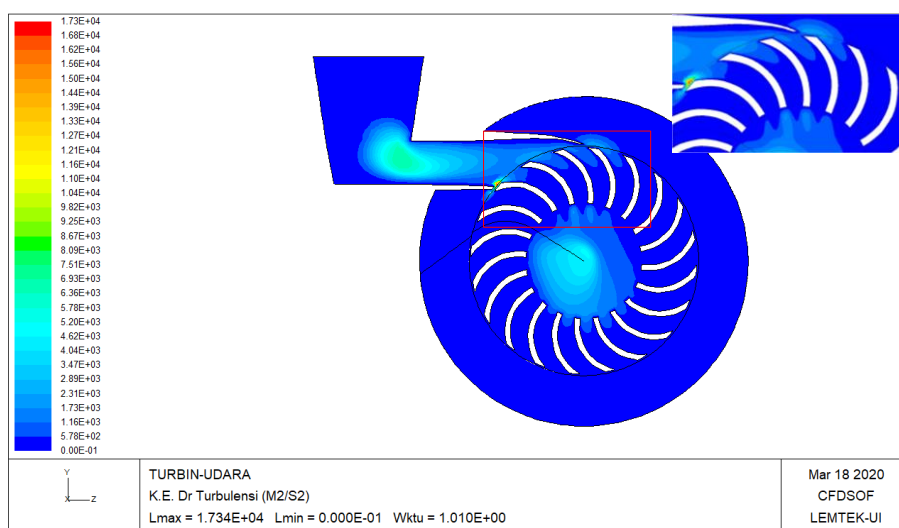


Fig. 6. The contour of turbulent kinetic energy

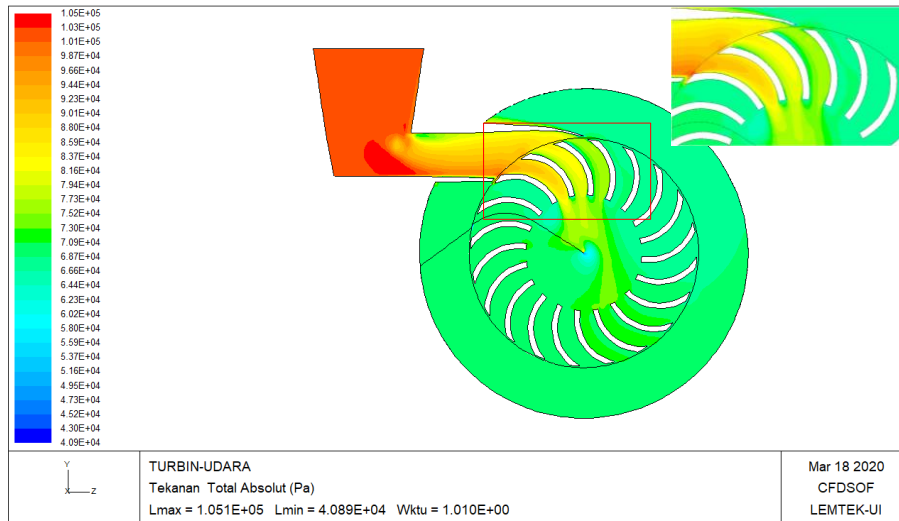


Fig. 7. The contour of absolute total pressure

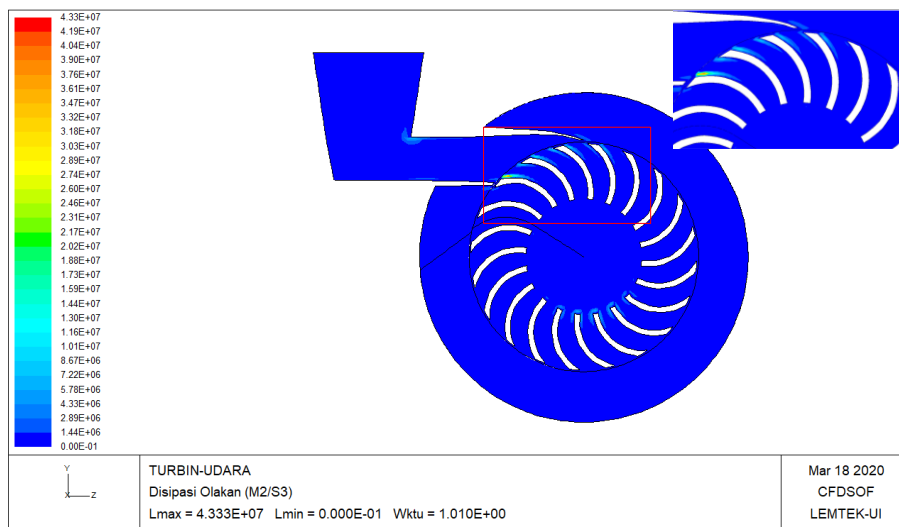


Fig. 8. The contour of turbulent dissipation rate

Simulation results show that in the surface area of the first stage blade inlet there is a large turbulent dissipation rate. This condition showing the change in σ_ϵ constant for the dissipation transport equation in the standard k- ϵ model will be sensitive to get results that are close to the RNG k- ϵ model. Figure 9 and Figure 10 show the static pressure and velocity curves from the inlet to the outlet of the first stage blade of crossflow turbine, respectively. The curve shows the sensitivity of the change in the constant σ_ϵ in the standard k- ϵ model to the average flow parameters of the distribution of static pressure and velocity. Likewise, the sensitivity of the constant change in the value of σ_ϵ for turbulent kinetic energy is shown in Figure 11.

Figures 12 and 13 show the turbulent dissipation rate curve and the turbulent effective viscosity from the inlet to the outlet of the first stage blade of crossflow turbine, respectively. Figures 12 and 13 revealed that the simulation results with the change in constant value $\sigma_\epsilon = 1.5$ standard k- ϵ model have a small deviation compared to the RNG k- ϵ model.

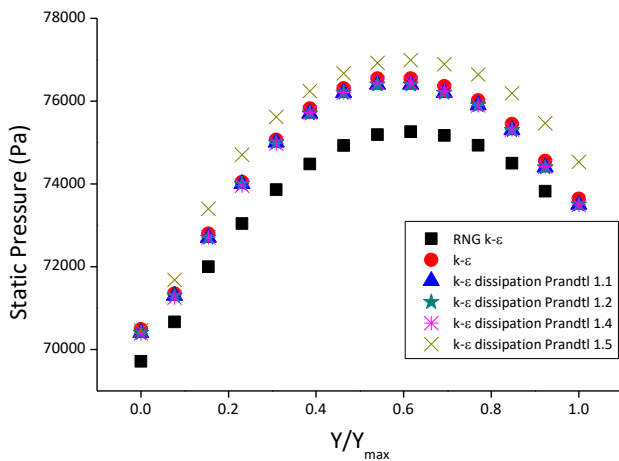


Fig. 9. Static pressure distribution along the y-axis of the crossflow turbine blade

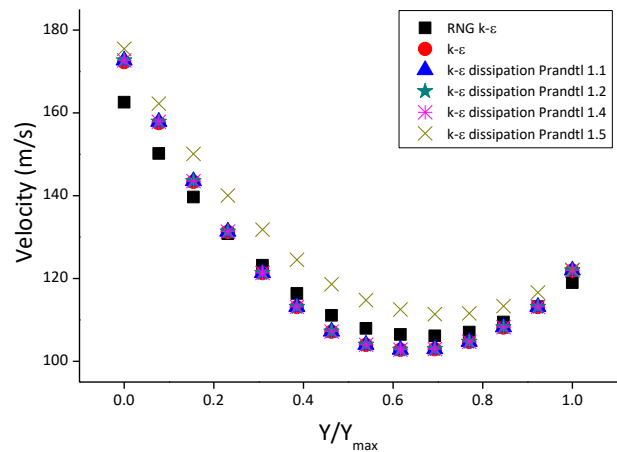


Fig. 10. Velocity distribution along the y-axis of the crossflow turbine blade

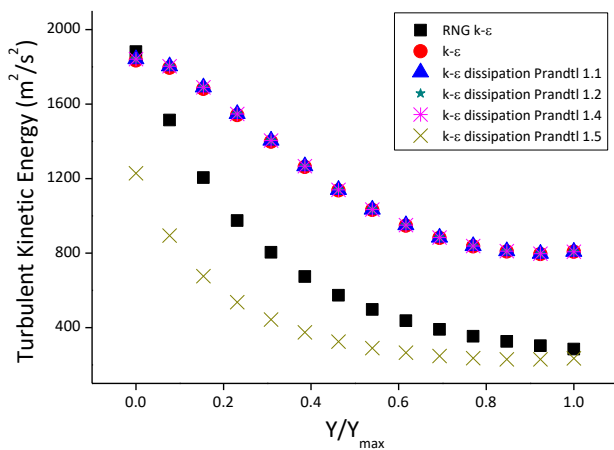


Fig. 11. Turbulent kinetic energy distribution along the y-axis of the crossflow turbine blade

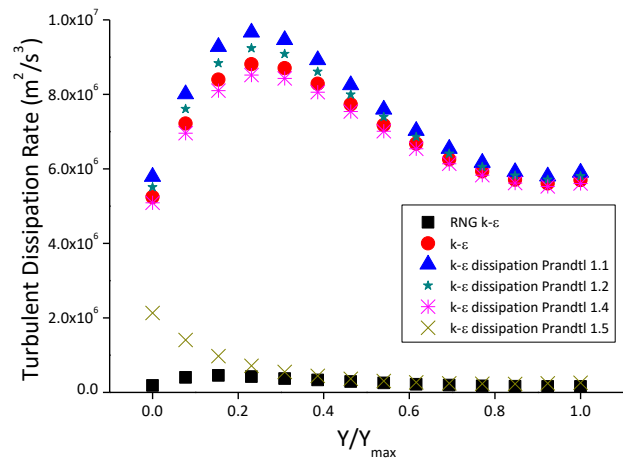


Fig. 12. Turbulent dissipation rate distribution along the y-axis of the crossflow turbine blade

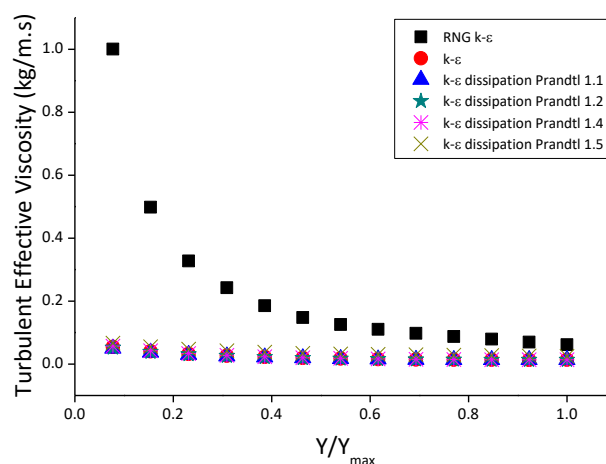


Fig. 13. Turbulent effective viscosity distribution along the y-axis of the crossflow turbine blade

The simulation results show that the constant value σ_ϵ standard k- ϵ model has a small deviation value to the RNG k- ϵ model (see Figures 11 and 12). This study recommends modifying the standard

k- ϵ model with changes in the constant $\sigma_\epsilon = 1.4$ to 1.5 to obtain results that are close to the RNG k- ϵ model.

4. Conclusions

Based on results, flow field prediction of cross-flow wind turbine using the standard k- ϵ model with constant σ_ϵ of 1.4 to 1.5 is the smallest deviation toward the RNG k- ϵ model. This shows that the constant σ_ϵ has an influence on the predictions of the flow field. So, to increase the accuracy of prediction constant σ_ϵ should be precisely defined.

Acknowledgment

The authors would like to thank the Directorate of Research and Service Community (DRPM) Universitas Indonesia for funding this research with grant number NKB.0152/UN2.R3.1/HKP.05.00/2019, and to PT. CCIT Group Indonesia for CFDSOF® software license.

References

- [1] Prakoso, Aji Putro, Ahmad Indra Siswantara, and Dendy Adanta. "Comparison between 6-DOF UDF and moving mesh approaches in CFD methods for predicting cross-flow pico-hydro turbine performance." *CFD Letters* 11, no. 6 (2019): 86-96.
- [2] Adanta, Dendy, Warjito Budiarmo, Ahmad Indra Siswantara, and Aji Putro Prakoso. "Performance comparison of NACA 6509 and 6712 on pico hydro type cross-flow turbine by numerical method." *Journal of Advanced Research in Fluid Mechanics and Thermal Sciences* 45, no. 1 (2018): 116-127.
- [3] Adanta, D., Emanuele Quaranta, and T. M. I. Mahlia. "Investigation of the effect of gaps between the blades of open flume Pico hydro turbine runners." *Journal of Mechanical Engineering and Sciences* 13, no. 3 (2019): 5493-5512. <https://doi.org/10.15866/jreme.v13i8.17453>
- [4] Siswantara, Ahmad Indra, Aji Putro Prakoso Budiarmo, Gun Gun R. Gunadi, and Dendy Warjito. "Assessment of Turbulence Model for Cross-Flow Pico Hydro Turbine Numerical Simulation." *CFD Letters* 10, no. 2 (2018): 38-48.
- [5] Tennekes, Hendrik, and John Leask Lumley. 1972. *A First Course in Turbulence*. MIT press.
- [6] Jehad, D. G., G. A. Hashim, A. K. Zaroor, and CS Nor Azwadi. "Numerical Study of Turbulent Flow over Backward-Facing Step with Different Turbulence Models." *Journal of Advanced Research Design* 4, no. 1 (2015): 20-27.
- [7] Adanta, Dendy, Warjito Budiarmo, and Ahmad Indra Siswantara. "Assessment of turbulence modelling for numerical simulations into pico hydro turbine." *Journal of Advanced Research in Fluid Mechanics and Thermal Sciences* 46, no. 1 (2018): 21-31.
- [8] Darmawan, Steven, Ahmad Indra Siswantara, Asyari Daryus Budiarmo, Agus Tri Gunawan, Achmad Bayu Wijayanto, and Harto Tanujaya. "Turbulent flow analysis in auxiliary cross-flow runner of a Proto X-3 Bioenergy micro gas turbine using RNG K- ϵ turbulence model." *ARPN Journal of Engineering and Applied Sciences* 10, no. 16 (2015): 7086-7091.
- [9] Versteeg, Henk Kaarle, and Weeratunge Malalasekera. *An introduction to computational fluid dynamics: the finite volume method*. Pearson education, 2007.
- [10] Mohammadi, Bijan, and Olivier Pironneau. "Analysis of the k-epsilon turbulence model." (1993).
- [11] Orszag, STEVEN A, and VICTOR Yakhot. "Renormalization Group Analysis of Turbulence." In *Proceedings of the International Congress of Mathematicians*, p. 1395-99, 1986.
- [12] Yakhot, Victor, and Steven A. Orszag. "Renormalization group analysis of turbulence. I. Basic theory." *Journal of scientific computing* 1, no. 1 (1986): 3-51. <https://doi.org/10.1007/BF01061452>
- [13] Klemm, Toni, Martin Gabi, and Jean-Nicolas Héraud. "Application of a cross flow fan as wind turbine." *Journal of Computational and Applied Mechanics* 8, no. 2 (2007): 123-133.
- [14] Gunadi, Gun Gun R., and Ahmad Indra Siswantara. "Turbulence models application in air flow of crossflow turbine." *International Journal of Technology* 9, no. 7 (2018): 1490-1497. <https://doi.org/10.14716/ijtech.v9i7.2636>
- [15] Fluent, A. N. S. Y. S. "ANSYS fluent theory guide 15.0." *Inc, Canonsburg, PA* (2013).

-
- [16] Yakhot, V. S. A. S. T. B. C. G., S. A. Orszag, Siva Thangam, T. B. Gatski, and C. G. Speziale. "Development of turbulence models for shear flows by a double expansion technique." *Physics of Fluids A: Fluid Dynamics* 4, no. 7 (1992): 1510-1520.
<https://doi.org/10.1063/1.858424>
- [17] Roache, Patrick J. *Verification and validation in computational science and engineering*. Vol. 895. Albuquerque, NM: Hermosa, 1998.